Available online at www.sciencedirect.com
ScienceDirect
Journal of Power Sources 179 (2008) 693–699
JOURNAL OF POWER SOURCES
www.elsevier.com/locate/jpowsour

Influence of micro-porous layer and operating conditions on the fluoride release rate and degradation of PEMFC membrane electrode assemblies

Sumit Kundu [a], Kunal Karan [b,*], Michael Fowler [a], Leonardo C. Simon [a], Brant Peppley [b], Ela Halliop [b]

[a] *Department of Chemical Engineering, University of Waterloo, 200 University Avenue West, Waterloo, Ontario, Canada, N2L 3G1*
[b] *Queen's-RMC Fuel Cell Research Centre, Kingston, Ontario, Canada, K7L 5L9*

Received 9 October 2007; received in revised form 26 November 2007; accepted 26 November 2007
Available online 16 January 2008

Abstract

In this study, the influence of micro-porous layers (MPL) on polymer electrolyte membrane fuel cell (PEMFC) durability was investigated. Two fuel cells were built, one with a micro-porous layer on the anode side, and a second cell with MPL on both sides. Experiments were conducted by varying operational parameters such as current density, reactant stoichiometry, and inlet relative humidity. Fuel cell degradation was evaluated by measuring fluoride release rates. The largest factor determining fluoride release rate was found to be the presence of MPL; the cell with MPLs on both sides exhibited significantly reduced fluoride release rates compared to that of cell with one MPL. Increasing the current density also reduced the fluoride release rate for cells with only one MPL whereas there was only a moderate effect on cells with two MPLs. Microscopy analysis showed small but significant changes in ionomer layer thickness. Polarization measurements indicated that there was little change in the performance for both cells over the test period.

Keywords: Micro-porous layer; Durability; Fluoride release; Membrane thinning

1. Introduction

Enhancing the durability of fuel cells is one of the key research and development goals currently being pursued to promote wide-scale commercialization of polymer electrolyte membrane fuel cell (PEMFC) technology. The membrane electrode assembly (MEA), and, in particular, the electrolyte membrane is considered to be one of the least durable components of a PEMFC. Accordingly, further understanding of how the MEA and the membrane degrade is much needed. The degradation process for fuel cells and related sub-components can be broadly summarized into causes, modes, and effects [1]. The causes resulting in the failure of polymer electrolyte membranes range from manufacturing and design to factors such as over-compression, MEA sub-component material, and electrolyte membrane thickness variability across the cell [2]. Material property effects such as electrolyte membrane swelling [3,4], and operating conditions such as sub-zero temperatures and extreme conditions of feed stream relative humidity [5–7] also cause degradation. Each cause results in a failure through a specific degradation mode, which can be classified as either mechanical, chemical, or thermal mode [1,2,8].

In recent studies by co-authors [9–11], it was observed that the presence of micro-porous layer (MPL) led to a remarkable improvement in the durability of fuel cells. A MPL is a composite of carbon particles and a hydrophobic agent that is coated on one side of the conventional gas diffusion media and can be used on one or both of the anode or cathode electrodes. Without conducting an analysis of the degradation, it was hypothesized that the MPL acted as a protective layer that prevented penetration of sharp carbon fibers into the membranes and, thereby, minimized or prevented mechanical damage of the membrane. Another possibility, which is a topic of this study,

* Corresponding author.
E-mail addresses: s2kundu@uwaterloo.ca (S. Kundu), kunal.karan@chee.queensu.ca (K. Karan).

0378-7753/$ – see front matter © 2008 Elsevier B.V. All rights reserved.
doi:10.1016/j.jpowsour.2007.11.117

is that the MPL itself affects the chemical degradation of the MEA.

Chemical degradation of the ionomer membrane generally leads to MEA failure by compromising the integrity of the membrane. In the case of perfluorosulfonic ionomer (PFSI) membranes such as Nafion^{TM}, it has been proposed that carboxylic acid end groups left over from the manufacturing process may be susceptible to attack by radical species [12] generated during fuel cell reactions. In particular, hydroxyl radicals are thought to be formed by the decay of hydrogen peroxide which itself is generated within the fuel cell. There is yet some debate as to whether peroxide is predominantly formed by hydrogen crossover, oxygen crossover or as an intermediate in the oxygen reduction reaction. Regardless of the exact mechanism for formation of H_2O_2, its existence in membrane leads to radical generation facilitating the degradation of the ionomer membrane [2,12–15] whose mechanism has been proposed as follows:

$$\text{Step 1}: \quad \text{R–CF}_2\text{COOH} + \text{OH}^\bullet \rightarrow \text{R–CF}_2^\bullet + \text{CO}_2 + \text{H}_2\text{O}$$

$$\text{Step 2}: \quad \text{R–CF}_2^\bullet + \text{OH}^\bullet \rightarrow \text{R–CF}_2\text{OH} \rightarrow \text{R–COF} + \text{HF}$$

$$\text{Step 3}: \quad \text{R–COF} + \text{H}_2\text{O} \rightarrow \text{R–COOH} + \text{HF}.$$

As shown above, hydrogen fluoride (HF) is a product of the membrane degradation reaction and may exit the fuel cell in the effluent water. In fact, fluoride ion release rates are often used as a measure of the membrane degradation rate.

Several factors are known to influence chemical degradation and include current density, relative humidity of the inlet streams, and cell temperature. OCV operation is thought to increase the rate of chemical degradation as a result of higher hydrogen and/or oxygen crossover [16–19]. In recent studies, it has been suggested that when an MEA is subjected to extended operation at OCV a platinum band may form in the membrane from an electrochemical deposition process and that degradation will occur within and near the band location [20–22]. A study by Pierpont et al. [23] examined the effect of three load profiles on the degradation of 3 M^{TM} MEAs and reported that the initial fluoride release was inversely correlated to MEA lifetime under the accelerated test conditions. They also reported that high relative humidity increased membrane durability but low average currents led to decrease in MEA lifetime.

There is a general consensus regarding the mechanism of chemical degradation of perfluorosulfonic ionomers leading to the formation of hydrogen fluoride. However, the extent to which the operating conditions such the inlet relative humidity and current density influence the ionomer degradation or affect the fluoride release rate is not completely understood. Furthermore, the role of MPL in enhancing fuel cell durability has not been examined in the context of membrane degradation.

As such, the primary objective of this study was to investigate the influence of MPL on the fluoride release rate, which is a measure of chemical degradation of ionomer membrane. To this end, two fuel cells, each with an MPL on the anode side but one with an additional MPL on the cathode, were studied. The influence of current densities was examined by measuring fluoride release rate at three current densities of 300 mA cm^{-2}, 500 mA cm^{-2} and 700 mA cm^{-2}. The effect of relative humidity was examined by conducting two sets of experiments wherein the anode/cathode relative humidity were maintained at 100%/60% and 60%/100%, respectively. Changes in ionomer membrane morphology were also investigated via scanning electron microscopy of MEAs.

2. Experimental

2.1. Materials and cell construction

A detailed description of the specific cell configuration and experimental test set-up is presented elsewhere [9–11]. Briefly, the cell had a 100 cm^2 active area using a catalyst coated membrane (CCM) from Ion Power Inc. The CCM for testing was used as-received without any additional processing steps. Two types of porous transport layer (PTL), commonly known as gas diffusion layers (GDL), were investigated—SGL 10BA and SGL 10BB carbon papers (SGL Carbon Group, Germany). Both SGL 10BA and 10BB carbon papers contain 5 wt% polytetrafluoroethylene (PTFE). The SGL 10BB carbon paper is essentially SGL BA paper with an additional functional layer – a micro-porous layer (MPL) – on one face. The PTFE content of the MPL was 23%. The thicknesses of the 10BA and 10BB carbon papers were 0.37 mm and 0.41 mm, respectively. Thus, it can be inferred that the micro-porous layer is 40 μm thick. The PTLs and the MEAs from the same batch were used in all the tests to minimize variability in the physical and chemical characteristics of the fuel cell components.

Two cell configurations were tested at different current densities, cathode stoichiometries, and cathode/anode relative humidity. The first cell configuration, herein referred to as Cell 1, used a PTL with an MPL on the anode side but no MPL on the cathode side. The second configuration, Cell 2, used PTL with MPL on both anode and cathode sides. For each cell, the cathode stoichiometry was either 2 or 3 and anode/cathode (A/C) relative humidity was adjusted to 100%/60% or 60%/100%. At each level of stoichiometry and relative humidity, the fluoride release rate measurements were made at current densities of 300 mA cm^{-2}, 500 mA cm^{-2}, and 700 mA cm^{-2}. The cell builds and test conditions are summarized in Table 1.

For each cell configuration, at each specific operating condition (A/C relative humidity, A/C stoichiometric ratio, and current density), the effluent water from the anode and cathode streams were collected and stored in polyethylene bottles for fluoride analysis.

2.2. Fluoride ion release

Fluoride ion analysis was carried out with a Dionex ED40 electrochemical detector working with a Dionex GP40 gradient pump. The minimum detectable fluoride ion concentration is 0.011 ppm F^-. The total time spent and the volume of water collected at each condition was used to determine effluent water flow rates which were then used with fluoride concentration measurements to determine the fluoride release rate.

Table 1
Summary of experimental conditions employed in this study

	Cathode MPL present	Anode/cathode relative humidity (RH)	Anode/cathode stoichiometric ratio	Current density (mA cm^{-2})
Cell 1	No	100/60	1.4/2	300
		60/100	1.4/3	500
				700
Cell 2	Yes	100/60	1.4/2	300
		60/100	1.4/3	500
				700

The total cumulative fluoride released for a cell was calculated as shown in (1)

$$F^-_{Tot} = \sum_i f^-_i T_i \quad (1)$$

F^-_{Tot} is the total (anode plus cathode) cumulative fluoride release, f^-_i the fluoride release rate for a set of conditions i, and T_i is the total time spent at a set of conditions.

2.3. Scanning electron microscopy (SEM)

SEM analysis was carried out using a LEO SEM with field emission Gemini Column. The gas diffusion layers were first removed from the membrane electrode assemblies. This was done by repeatedly heating/humidifying and then cooling the MEA until the GDL could be removed easily. Samples of catalyst coated membrane (CCM) were cut into squares of approximately 0.5 cm × 0.5 cm and fixed to an aluminum stub with double sided conductive tape. Cross-sections were made by freeze fracture from a strip of sample submerged in liquid nitrogen. Once frozen, the sample was broken in half while still submerged. Samples were also sputter coated with gold to improve conductivity.

Average membrane thickness estimates were obtained by imaging catalyst coated membrane (CCM) cross-sections from 6 locations over the active area. Several images were taken at different points of the cross-sections and thickness was measured at more than 5 areas of each image with Scion Image Analysis software to produce an estimate of CCM thickness.

3. Results and discussion

The influence of MPL (i.e. presence or absence on the cathode side) and the effects of three operational factors – current density, relative humidity, and stoichiometry – on fluoride release rates were examined. Base case operating conditions were an anode/cathode stoichiometry of 1.4/3.0 and anode/cathode RH of 100%/60% while the base case cell configuration uses an MPL on the anode and no MPL on the cathode.

3.1. Fluoride release rate for base case conditions

The base case results in terms of fluoride release rate as a function of current densities is presented in Fig. 1. It is worth noting that the ensuing discussion is based on the results of a limited number of current density data points. Nonetheless, these results allow observation of overall trends and offer important insights into the effect of current density on membrane degradation. From Fig. 1, it can be noted that the fluoride emission rate decreases with an increase in current density. A large change in fluoride release rate from 4.2 μmol h^{-1} to 1.0 μmol h^{-1} was observed as the current density was increased from 300 mA cm^{-2} to 500 mA cm^{-2}. A much smaller change occurs as the current density was further increased from 500 mA cm^{-2} to 700 mA cm^{-2} with fluoride release rate decreasing to 0.7 μmol h^{-1}. This is consistent with the finding of Pierpont et al. [23] who used PTL without MPLs. In the present study, since experiments at different current densities were conducted with the same membrane in one continuous experiment, some of the variability in the results as indicated by the error bars is due partially to time effects since the fluoride emission rate increased with age.

As discussed, chemical degradation is typically linked to the crossover of gases from one side to the other in a fuel cell [16–18]. In recent modeling work the change in hydrogen crossover rate with current density was estimated by Rama et al. [24]. They showed that with an increase in current density the rate of hydrogen crossover will decrease. Thus, it may be expected that the chemical degradation (fluoride release rate) will decrease with increasing current density.

The fluoride release rate from the anode and the cathode electrodes are also shown in Fig. 1. Clearly, the anode and cathode fluoride release results are significantly different. First, the cathode fluoride release rates ranging 4.1 μmol h^{-1} (300 mA cm^{-2}) to 0.4 μmol h^{-1} (700 mA cm^{-2}) are higher than those from

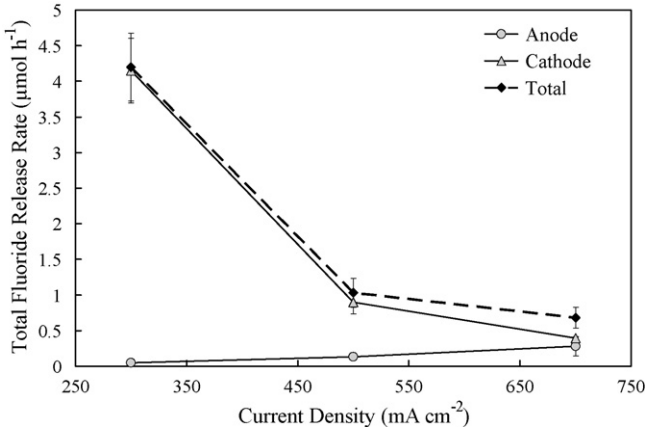

Fig. 1. Anode, cathode and total fluoride release rate as a function of current density for the Cell 1 basecase. [A/C stoichiometric ratio = 1.4/3; A/C RH = 100/60 anode/cathode; MPL only on anode side].

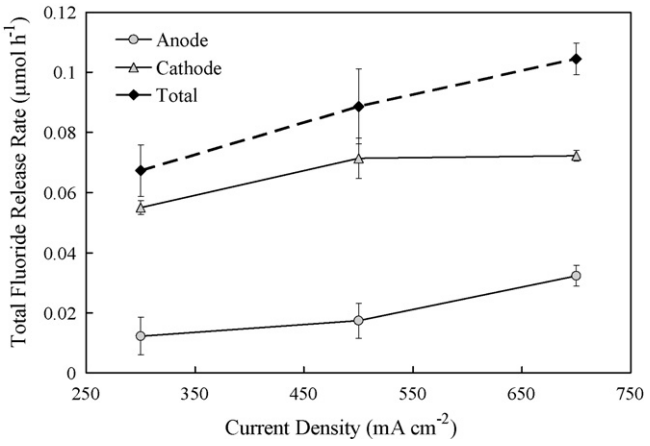

Fig. 2. Anode, cathode and total fluoride release rate versus current density for the cell 2. [A/C stoichiometric number 1.4/3 and RH 100/60. MPL on cathode and anode sides].

the anode which range from 0.05 μmol h^{-1} (300 mA cm^{-2}) to 0.28 μmol h^{-1} (700 mA cm^{-2}). The second major difference is that with an increasing current density the cathode fluoride release decreases while the anode release increases. To explain the higher fluoride release rate at the cathode compared to that at the anode, two factors must be considered—the location of the degradation, and the net transport of water from anode to cathode or vice-versa. The location of degradation can influence release rates on the anode and the cathode by influencing the path resistance that fluoride ions must overcome when diffusing from the generation point to either the anode or the cathode channels. Thus, if degradation occurs closer to the cathode ionomer/catalyst-layer interface, then the fluoride will preferentially diffuse out to the cathode channels because of the shorter path length or the lower diffusional resistance. The direction of net water transport in our experiments, as presented in our published studies [9,10], is from the anode to the cathode. As such, the fluoride ions may be convectively transported to the cathode from the generation point. Now, the decrease in cathode fluoride release rate with current density can be attributed to lower rate of membrane degradation due to decrease in reactant crossover as discussed above. The slight increase in anode fluoride release rate may be attributed to the decrease in water drag from the anode to the cathode. The data for water drag, presented in Atiyeh et al. [10], for the corresponding experiments show a slight decrease in water drag, however, the variability in water drag data is large enough to establish a definitive trend.

3.2. Influence of MPL on fluoride release rate

The addition of a second MPL to the cathode side of the membrane, in Cell 2, causes several changes to the degradation rates as measured by fluoride release. Total fluoride release rate is shown in Fig. 2 where it is immediately clear that the addition of the second MPL to the cathode has reduced the overall fluoride emission rate by 1 or 2 orders of magnitude compared to that for the base case. Fluoride release rates with Cell 2 ranged from 0.067 μmol h^{-1} at 300 mA cm^{-2} to 0.104 μmol h^{-1} at 700 mA cm^{-2}. The second difference between Cell 1 and Cell 2 is that the general trend with current density is different. For Cell 1, there were significant differences in fluoride release rate from low to high current densities, however, for Cell 2 the total fluoride release rates are similar after accounting for the experimental variability although a slight overall increasing trend rather than a decreasing trend is observed.

Although it is not entirely clear why the addition of the MPL had such a significant effect on fluoride release rate it is possible that the MPL impacts the rate of crossover of gases by impeding the diffusion of gases to the catalyst layer and, thereby, decreasing the driving force for diffusion across the ionomer membrane. It is also unclear why the degradation rate may increase with an increase in the current density, although the increase in the fluoride emission rate may be related to the water content of the catalyst layer and the MPL at these different current densities. It should also be noted that the changes with current density is not very significant and may be an artefact of a second degradation process. As alluded to earlier, the variability in the data is caused by both the experimental variability and the aging effects.

Anode and cathode fluoride release rate trends are also somewhat different from the baseline trends as shown in Fig. 2. Similar to the baseline, cathode fluoride release is higher than anode fluoride release though not as significantly; 0.055–0.072 μmol h^{-1} (700 mA cm^{-2}) on the cathode and 0.011 μmol h^{-1} (300 mA cm^{-2}) to 0.032 μmol h^{-1} (700 mA cm^{-2}) on the anode. This is again attributed to the fluoride generation point being closer to the cathode ionomer/catalyst interface and due to water drag being predominantly towards the cathode.

3.3. Morphological and electrochemical analysis

Membranes in Cell 1 (with no MPL on cathode) and Cell 2 (with MPL on cathode and anode) were further examined with scanning electron microscopy (SEM) to investigate morphological changes. Typical SEM images of membrane cross-sections are shown in Fig. 3a (Cell 1) and Fig. 3b (Cell 2). Comparison of the thicknesses revealed that there was a small difference between the two membranes. The membrane in Cell 1, which ran for a total of 729 h, had an average thickness of 43 μm while the membrane in Cell 2, which ran for 525 h, had a thickness of 50 μm. The nominal thickness of the membrane is 50.8 μm indicating that the membrane run with only one MPL thinned more than the membrane with two MPLs. This agrees with the fluoride release rates observed for this cell and more importantly with cumulative fluoride release. For Cell 1 the total cumulative fluoride lost per geometric active area was 10.1 μmol cm^{-2} and Cell 2 only lost 0.5 μmol cm^{-2}. Using the thickness measurements it can be estimated that for every 100 μmol of fluoride released per cm^2 of active area there was a thickness change of approximately 0.01 μm. The SEM analysis also showed no evidence of the formation of a platinum band.

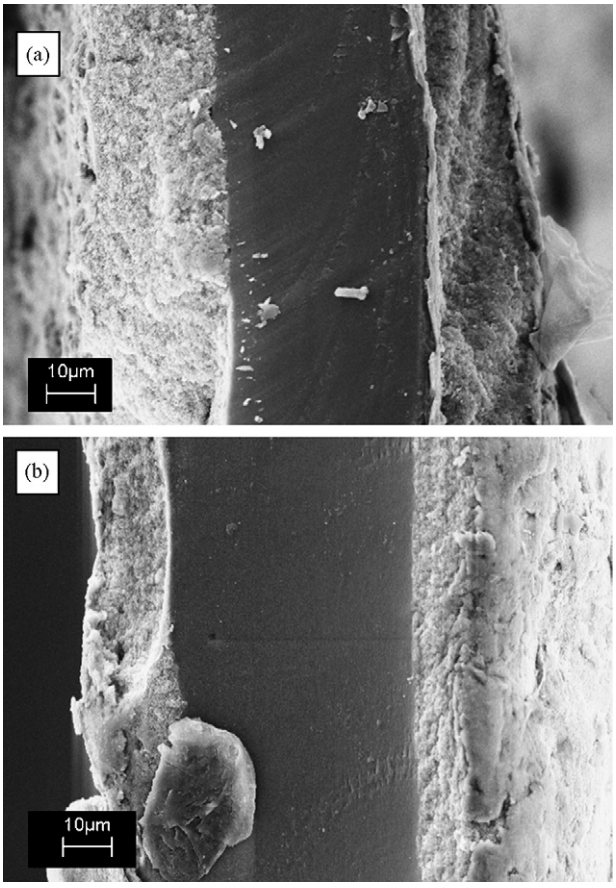

Fig. 3. SEM cross-section images of catalyst coated membranes used for (a) Cell 1 (no cathode MPL) and (b) Cell 2 (with cathode MPL).

3.4. Polarization behaviour

As a measure of the electrochemical performance, polarization data was obtained at the standard conditions of 100% RH for both anode and cathode feed streams and anode and cathode stoichiometric ratios of 1.4 and 3.0, respectively. The polarization behaviour for both fuel cell builds (Cell 1 and Cell 2) at the beginning-of-life (BOL) (30 h and 28 h, respectively) and end-of-life (EOL) (665 h and 529 h, respectively) are shown in Fig. 4. Both cells had similar performance at BOL and EOL. Cell 1 (MPL at anode only) shows slightly better performance at EOL. This is attributed to additional break-in effects after the BOL curve measurements. Additional measurements for Cell 1 at 228 h, 359 h, and 406 h (not shown for simplicity) indicate no significant change in performance for Cell over the testing period. This is also true of Cell 2. In general the overall polarization behaviours are similar for both cells and exhibit little effect of aging on the performance.

The above results are consistent with the forensic data that indicated a slight reduction in thickness for the one MPL case. The impact of the thickness change on voltage can be estimated using Eq. (2):

$$\eta_{ix} = -\frac{RT}{F} \ln\left[\frac{i_{crossover}}{10(L_{ca}A_{Pt,el})i_0}\right] \quad (2)$$

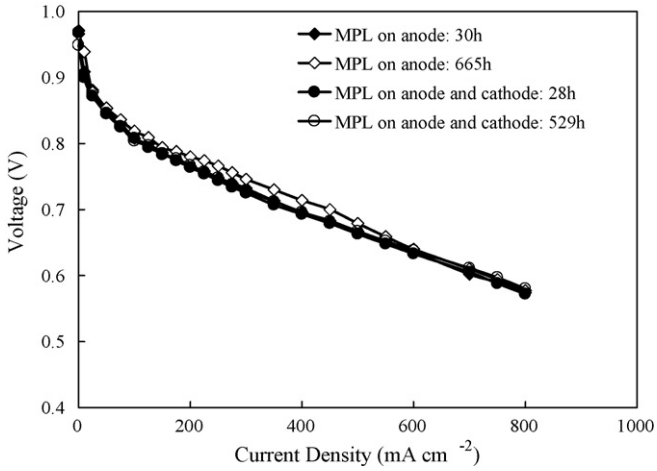

Fig. 4. Polarization curves for Cell 1 at BOL (30 h) and EOL (665 h) and for Cell 2 at BOL (28 h) and EOL (529 h).

where η_{ix} is the voltage loss due to hydrogen crossover, R the ideal gas constant, T the cell temperature, F the Faraday's constant, $i_{crossover}$ is the hydrogen crossover current, L_{ca} is the catalyst loading, $A_{pt,el}$ is the specific platinum surface area, and i_0 is the exchange current density.

Assuming no change in electrochemically active surface area, which is likely valid for small amounts of degradation, the influence of the change in thickness can be estimated the difference in voltage from two times, t_1 and t_2, can be given by Eq. (3):

$$\Delta E_{OCV} = -\frac{RT}{F} \ln\left[\frac{i_{crossover,t_2}}{i_{crossover,t_1}}\right]. \quad (3)$$

Further the crossover current is related to the molar flux of hydrogen crossing over which can be related to the inverse of the membrane thickness from Fick's law as shown in Eq. (4):

$$i_{crossover} \alpha N_{H_2} \alpha \frac{1}{\delta_m}. \quad (4)$$

Combining (4) and (3) can provide an estimate on the impact to open circuit voltage from a reduction in membrane thickness as shown in Eq. (5):

$$\Delta E_{OCV} = -\frac{RT}{F} \ln\left[\frac{\delta_{m,t_1}}{\delta_{m,t_2}}\right]. \quad (5)$$

For the thickness decrease of 7.8 μm for the fuel cell with 1 MPL and 0.8 μm for the fuel cell with 2 MPL Eq. (5) predicts a change in voltage of −4.8 mV and −0.5 mV, respectively. These differences fall within the experimental variability of the measured polarization curves.

3.5. Impact of anode/cathode stoichiometry and anode/cathode relative humidity

The effect of changing the anode/cathode stoichiometry from 1.4/3 to 1.4/2 was also explored, as was changing the anode/cathode relative humidity from 100%/60% to 60%/100%. The results for all four combinations of stoichiometry and RH for Cell 1 and Cell 2 are shown in Fig. 5a and b, respectively.

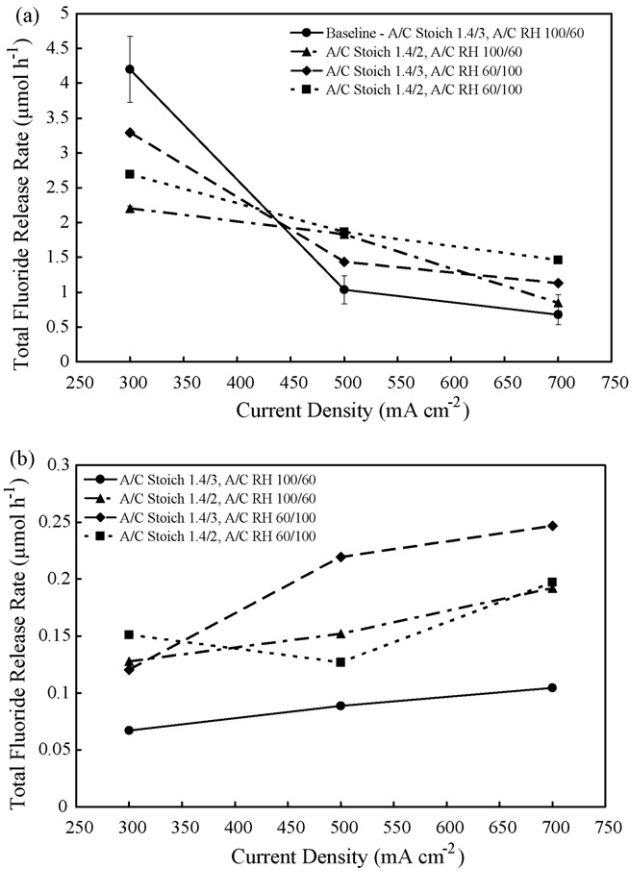

Fig. 5. Impact of cathode stoichiometry and anode/cathode RH on total fluoride release rate for (a) Cell 1 (no cathode MPL) and (b) Cell 2 (with cathode MPL).

No conclusive trends can be identified at this time as changes in the factors produce inconsistent results. An example of one such issue is that at low current densities (300 mA cm^{-2}) the fluoride release rates can be organized by cathode stoichiometries where high stoichiometry resulted in the highest fluoride release rates irrespective of the RH conditions. However at higher current densities of 700 mA cm^{-2} the fluoride results show that low anode RH produce the highest release rates. Further, within each RH set, a lower cathode stoichiometry produced higher fluoride release. With the addition of the second MPL on the cathode the fluoride release results follow entirely different trends compared to the baseline case.

4. Conclusions

The influence of micro-porous layer on the ionomer degradation via a chemical degradation mode was studied by observing trends in fluoride release rates from a PEMFC. Two cell constructions were examined: one using a single MPL on the anode side but none on the cathode, and a second cell configuration using MPLs on both the anode and cathode. Several operational conditions were examined such as current density, anode/cathode stoichiometry and relative humidity.

Under the baseline conditions (anode/cathode stoichiometry of 1.4/3 and anode/cathode RH of 100%/60%) and only one MPL on the anode the total fluoride release rate was observed to decrease with increasing current density. This was attributed to reduction in hydrogen crossover at higher currents. Cathode fluoride release was higher than anode release which is thought to be due to degradation being close to the cathode catalyst/ionomer interface as well as convective transport of water from anode to the cathode. Changes in water drag characteristics were responsible for decreasing cathode fluoride release and increasing anode fluoride release with increasing current density.

The addition of the second MPL dramatically reduced the total fluoride release rate compared to the baseline case by an order of magnitude. Cathode release was still higher than anode fluoride release however trends with current density differed.

Analysis of the morphology of the membranes revealed that the MEA with only one MPL had a thinner membrane than that with MPLs on both electrodes. The membrane in the baseline construction showed thinning of approximately 7.8 μm and a total cumulative fluoride release of 10.1 μmol cm^{-2} while the MEA with two MPLs had a 0.8 μm decrease in thickness and a fluoride loss of 0.5 μmol cm^{-2}. Calculations indicate that both thickness changes would result in a voltage drop that was within experimental variability as a result of the increased hydrogen crossover. This was consistent with polarization curve measurements throughout the cell life. Changes in cathode stoichiometry and relative humidity did not correlate well with fluoride release measurements.

Acknowledgements

The authors would like to acknowledge Ion Power Inc. for supporting this study and the Natural Sciences and Engineering Research Council (NSERC) of Canada for financial support.

References

[1] S. Kundu, M.W. Fowler, L.C. Simon, S. Grot, J. Power Sources 157 (2006) 650–656.
[2] A.B. LaConti, M. Hamdan, R.C. McDonald, in: W. Vielstich, H. Gasteiger, A. Lamm (Eds.), Handbook of Fuel Cells—Fundamentals, Technology and Applications, vol. 3, John Wiley & Sons, New York, 2003, pp. 647–663.
[3] C.H. Paik, T. Skiba, V. Mittal, S. Motupally, T.D. Jarvi, Proceedings of the 207th Meeting of the Electrochemical Society—Meeting Abstracts, 2005, 771.
[4] M.F. Mathias, R. Makharia, H.A. Gasteiger, J.J. Conley, T.J. Fuller, C.J. Gittleman, S.S. Kocha, D.P. Miller, C.K. Mittelsteadt, T. Xie, S.G. Yan, P.T. Yu, Electrochem. Soc. Interface 14 (2005) 24–36.
[5] Q. Guo, Z. Qi, J. Power Sources 160 (2006) 1269–1274.
[6] E. Endoh, S. Terazono, H. Widjaja, Y. Takimoto, Electrochem. Solid-State Lett. 7 (2004) A209–A211.
[7] J. St Pierre, D.P. Wilkinson, S. Knights, M.L. Bos, J. New Mater. Electrochem. Syst. 3 (2000) 99–106.
[8] A. Collier, H. Wang, X. Zi Yuan, J. Zhang, D.P. Wilkinson, Int. J. Hydrogen Energy 31 (2006) 1838–1854.
[9] K. Karan, H. Atiyeh, A. Phoenix, E. Halliop, J. Pharoah, B. Peppley, Electrochem. Solid-State Lett. 10 (2007) B34–B38.
[10] H.K. Atiyeh, K. Karan, B. Peppley, A. Phoenix, E. Halliop, J. Pharoah, J. Power Sources 170 (2007) 111–121.
[11] J.G. Pharoah, B. Peppley, H. Atiyeh, E. Halliop, K. Karan, A. Phoenix, ECS Trans. 3 (1) (2006) 1227–1237.
[12] D.E. Curtin, R.D. Lousenberg, T.J. Henry, P.C. Tangeman, M.E. Tisack, J. Power Sources 131 (2004) 41–48.

[13] A. Panchenko, H. Dilger, J. Kerres, M. Hein, A. Ullrich, T. Kazc, E. Roduner, Phys. Chem. Chem. Phys. 6 (2004) 2891–2894.
[14] M. Inaba, Proceedings of the 14th International Conference on the Properties of Water and Steam in Kyoto, 2005, pp. 395–402.
[15] J. Healy, C. Hayden, T. Xie, K. Olson, R. Waldo, H. Gasteiger, J. Abbott, Fuel Cells 5 (2005) 302–308.
[16] M. Aoki, H. Uchida, M. Watanabe, Electrochem. Commun. 8 (2006) 1509–1513.
[17] J.J.A. Kadjo, J.P. Garnier, J.P. Maye, F. Relot, S. Martemianov, Russ. J. Electrochem. 42 (2006) 467–475.
[18] V.O. Mittal, H.R. Kunz, J.M. Fenton, J. Electrochem. Soc. 153 (2006) 1755–1759.
[19] T. Kinumoto, M. Inaba, Y. Nakayama, K. Ogata, R. Umebayashi, A. Tasaka, Y. Iriyama, T. Abe, Z. Ogumi, J. Power Sources 158 (2006) 1222–1228.
[20] H. Liu, J. Zhang, F.D. Coms, W. Gu, B. Litteer, H.A. Gasteiger, ECS Trans. 3 (2006) 493–505.
[21] A. Ohma, S. Suga, S. Yamamoto, K. Shinohara, ECS Trans. 3 (2006) 519–529.
[22] A. Ohma, S. Suga, S. Yamamoto, K. Shinohara, J. Electrochem. Soc. 154 (2007) 757–760.
[23] D. Pierpont, M. Hicks, T. Watschke, P. Turner, ECS Trans. 1 (2005) 229–237.
[24] P. Rama, R. Chen, R. Thring, Proc. Inst. Mech. Eng. Part A: J. Power Energy 220 (2006) 535–550.